Available online at www.sciencedirect.com
SCIENCE DIRECT®
Thermochimica Acta 408 (2003) 9–16
thermochimica acta
www.elsevier.com/locate/tca

Domain analysis of human apotransferrin upon interaction with sodium *n*-dodecyl sulphate: differential scanning calorimetry and circular dichroism approaches

M. Rezaei-Tavirani [a,b], A.A. Moosavi-Movahedi [a,*], S.Z. Moosavi-Nejad [a], J. Chamani [a], D. Ajloo [a]

[a] *Institute of Biochemistry and Biophysics, University of Tehran, P.O. Box 13145-1384, Tehran, Iran*
[b] *Faculty of Medicine, Medical University of Ilam, Ilam, Iran*

Received 26 June 2002; received in revised form 14 April 2003; accepted 16 May 2003

Abstract

The domain analysis of human apotransferrin (apo hTF) upon interaction with sodium *n*-dodecyl sulphate (SDS) was studied by differential scanning calorimetry (DSC) and circular dichroism (CD) using Hepes buffer, 100 mM, at pH = 7. The DSC profile for apo hTF depicts two distinct peaks, while when interacted with SDS, the DSC peaks are shifted to the left as well as the area under the peaks are reduced. The DSC profile without the presence of SDS has two dissimilar peaks including two melting points ($T_m = 60\,^{\circ}C$, $T_m = 70\,^{\circ}C$). This profile in the presence of low concentrations of SDS shows two nearly similar peaks and decrement of T_m values about 5 °C relative to profile in the absence of SDS. The DSC excess heat capacity was deconvoluted for apo hTF in the presence of SDS. The interaction of SDS with apo hTF induced two dissimilar subdomains for each domain, but each domain having two subdomains similar to each other. The CD experiment of apo hTF–SDS complexes shows the decrement of α-helix content and the increment of β-sheet structure relative to protein in the absence of SDS. The α-helix tendency calculation shows more α-helix content for N domain relative to C domain. Here SDS at low concentration plays a role as a good probe to define the electrostatic moiety for N domain relative to C domain that is initiated from dissimilarity of α-helicity of two domains.

Keywords: Human apotransferrin; Electrostatic interaction; Domain analysis; Sodium dodecyl sulphate; Differential scanning calorimetry

1. Introduction

The binding of surfactants to water-soluble proteins [1–3] and the structural elucidation of protein denaturation by surfactants [4–7] have been studied extensively. Sodium *n*-dodecyl sulphate (SDS) as an anionic surfactant including one polar head (sulphate group) and hydrophobic tail (aliphatic chain, contain 12 carbon atoms), is a potent probe for analysis of the protein structure [8–12]. It is generally accepted that binding of surfactant molecule to protein occurs by combination of ionic and hydrophobic interactions [13,14]. The protein–SDS complexes in the range of electrostatic portion may induce the conformational change while SDS in high concentration cause the unfolding for protein [15].

Transferrins are the classes of the protein that bind to the two Fe^{3+} ions and finally supply them to

* Corresponding author. Tel.: +98-21-6403957; fax: +98-21-6404680.
E-mail address: moosavi@ibb.ut.ac.ir (A.A. Moosavi-Movahedi).

0040-6031/$ – see front matter © 2003 Elsevier B.V. All rights reserved.
doi:10.1016/S0040-6031(03)00311-3

metabolising cells [16–18]. Human transferrin (hTF) is a single subunit protein containing 678 amino acid residues [19], including two domains called C and N domains which are further divided into two similarity sized lobs [20]. The binding site of each domain is located in the cleft between two lobes of domain. The two domains of hTF show about 40% homology with similar tertiary structure but not identically. Crystal structures of the diferric forms [21,22] and the monoferric N domain [23] of several transferrins indicate that the two lobs are closed over one Fe^{3+} ion.

For the ion-free apo form, all of the transferrin domains, except for the lactoferrin C domain in crystal, assume a conformation with an opening of the interlobe cleft [24,25] implied that transferrin initially binds the Fe^{3+} ion in the open form before being transformed into the closed holo form [26]. But Mizutani et al. [27] have shown a novel structural state of transferrin: the Fe^{3+}-loaded structure of ovotransferrin N domain with essentially the same open atom conformation as the apo form. Studies on ovotransferrin showed clearly that both the free energy and heat of interaction of the two domains were quite dependent on whether neither one nor both had an attached ferric ion [28]. On the other hand, the binding of diferric transferrin to its receptor apparently depends on the two-domain structure of these proteins [29,30]. Therefore, it seems that iron-dependent changes in domain–domain interactions may produce changes in the structure of transferrin, which are required for proper interaction with receptors in order to carry out the final physiological function [31].

The kinetic approaches have shown that the N domain was saturated by Fe^{3+} ion after complete saturation of C domain [32]. Differential scanning calorimetric (DSC) studies has shown that C and N domains of apo hTF were unfolded separately, with melting point (T_m) 69 and 78 °C, respectively. The hTF undergoes conformational changes during iron binding, so the value of the T_m for both C and N domains alter to 90 °C [31,33]. Domain interactions for ovotransferrin are larger than serum transferrin, therefore two domains of serum transferrin show separated transition in DSC profiles, but two domains of ovotransferrin appear as a single transition [31]. In this paper we attempt to obtain the additional information for C and N domains, due to interaction of SDS at the low concentration (in the range of electrostatic interaction) with apo hTF, through DSC and CD techniques.

2. Materials and methods

2.1. Materials

Apotransferrin and SDS were obtained from Sigma. The other substances of reagent grade were obtained from Merck. The buffer used through out the study was Hepes 100 mM, and pH = 7.0.

2.2. Methods

DSC experiment was carried out on a Scal-1 microcalotimeter (Russia), the heating rate was fixed at 1 K/min. An extra pressure of 1.5 atm was maintained during all DSC runs to prevent possible degassing of the solutions on heating. The deconvolution analysis and fitting were done based on Privalov and Potekhin theory [34] which was installed as DOS program in software package (named Scal-2) and supplied by Scal (Russia). Scal-2 program, which is installed in DSC instrument, enables to determine the native and denatured lines based on excess C_p. This program enables to deconvolute the C_p excess profile to the corresponding subpeaks based on fitting error. The best fitting error is selected as a best deconvolution (in this work the best fitting error equal to 0.8%).

Recommendation for the best fitting procedure that is accommodated in Scal-2 program is as follows:

- Specifying of the appropriate native and denature linear lines.
- Determination of the excess heat capacity function.
- Intrinsic heat capacity is extracted from excess heat capacity function.
- Minimising the following function, assuming the most probable number of states which defined as i:

$$\phi(\Delta_0^i H, \Delta_0^i S, \Delta_0^i C_p, n) = \int_0^\infty [\langle \Delta C_p(T) \rangle_{\text{Theor}} - \langle \Delta C_p(T) \rangle \exp]^2 \, dT$$

- If the experimental curve cannot be approximated by the calculated one, increase the experimental one (alternation of i to determine the optimum fitting),

eliminate the states with a low maximal population and repeat the minimisation.

The baseline preparation was done by buffer including 0.5 mM SDS in both sample and reference cells.

CD spectra were recorded on a Jasco J-715 spectropolarimeter (Japan). Results are expressed as ellipticity, $[\theta]$ ($^\circ$ cm^2 dmol^{-1}), based on a mean amino acid residue weight (MRW) assuming the average weights 118 D for transferrin. The molar ellipticity was determined as $[\theta]_\lambda = (\theta \times 100\,\mathrm{MRW}/cl)$, where c is the protein concentration in mM, l the light path length in cm and θ the measured ellipticity in degree at a given wavelength. The data was smoothed using the Jasco J-715 software, including the fast Fourier-transform noise reduction routine, which allows enhancement of most noisy spectra without distorting their peak shapes. All experiments were repeated three times. The molecular weight of transferring is 80 000 Da, the concentration of the protein solution was 1 mg/ml (0.0125 mM) and 1.2 mg/ml (0.015 mM) for DSC and CD experiments, respectively. It is worthy to note the DSC profile shows the reversible process for the protein concentration of 0.0125 mM in the presence of 0.5 mM SDS, whereas the higher concentration of SDS (12 mM) or protein (5 mg/ml) caused the irreversibility (aggregative process).

Percentage of secondary structures was calculated by Chen et al. method [35]. The rotatory contributions of a protein can be determined by $X = f_\mathrm{H}X_\mathrm{H} + f_\beta X_\beta + f_\mathrm{R}X_\mathrm{R}$ where X can be either the ellipticity or the rotation at any wavelength. f is the fractions of the helix (f_H), beta form (f_β) and unordered form (f_R); the sum of f is equal to unity and each f is greater than or equal to zero. With the f values of five proteins obtained by X-ray diffraction studies, the X of the protein at any wavelength is fitted by a least-squares method, which defines the X_H, X_β and X_R. The circular dichroism (CD) for the helix, beta and random forms determined thus can be conversely used to estimate the secondary structure of any protein with X at several wavelengths for the same equation. The α-helical content (f_H) was estimated from the ellipticity value at 222 nm ($[\theta]_{222}$) as described as follows [35]:

$$f_\mathrm{H} = -\left([\theta]_{222} + \frac{2340}{30\,300}\right)$$

Average hydrophobicity, $\langle H_\phi \rangle$ [36] and average helix propensity, $\langle H_\mathrm{D} \rangle$ [36] were calculated as follows:

$$\langle H_\phi \rangle = \sum \frac{(H_\phi)_i n_i}{N} \quad (1)$$

$$\langle H_\mathrm{D} \rangle = \sum \frac{(H_\mathrm{D})_i n_i}{N} \quad (2)$$

N, H_ϕ, H_D and n_i are total number of amino acids, hydrophobicity, helix propensity belonging to amino acid of type i, and number of amino acid of type i, respectively. The hydrophobicity and helix propensity data were used from literature [36,37].

3. Results and discussion

Fig. 1 represents CD spectra of apo hTF in the presence of different concentrations of SDS. The spectra (curves 2, 3 see legend) in the low concentrations of SDS were shifted to the left relative to the spectrum of protein without the presence of SDS at wavelength 200–220 nm (curve 1). The left shift and reduction of CD ellipticity ($-\theta_{222}$) indicating the decrement of α-helix and increment of β-sheet contributions in secondary structure of apo hTF due to effect of SDS. The extent relation of peaks at 208–222 nm shows the secondary classes of the protein. The 208 nm band is larger than the 222 nm band for the curves 1, 2 and 3, therefore, relative ratio of the 208 nm band to the 222 nm band is larger than 1. This indicates the CD spectra (curves 1, 2 and 3) of apo hTF in the absence and presence of SDS are α+β structural type. Usually proteins have been divided into five structural classes on the base of their secondary structure [38,39]: all α, all β, α + β (separated α-helix and β-sheet regions), α/β (intermixed α and β region) and random. In the α + β type the 208 nm band is larger than the 222 nm band, while the relative intensities are reversed in α/β proteins [38,40]. Curve 4 shows the decrement of secondary structures (α-helix and β-sheet) due to higher concentration of SDS that may accompany with denaturation. The percentage of secondary structures of apo hTF in the presence of different concentrations of SDS is recorded in Table 1. Our results show the amount of α-helix, β-sheet and other structure without the presence of SDS are equal to 32.6, 28.3 and 39.1%, respectively. These results are also consisted

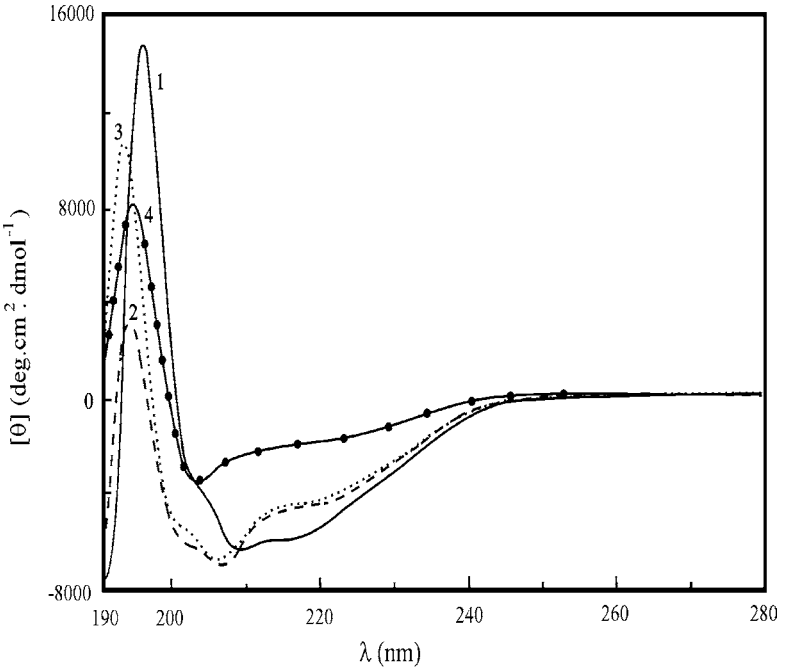

Fig. 1. Far-UV CD spectra (ellipticity, θ) of apo hTF in the absence of SDS (solid line, curve 1) and in the presence of 0.5 mM (dashed line, curve 2), 1 mM (pointed line, curve 3) and 9 mM (filled circle, curve 4) concentrations of SDS.

with literature [41]. Due to the effect of low concentrations of SDS (0.5–1.5 mM SDS) upon interaction with apo hTF the amount of α-helix is reduced, whereas the amount of β-sheet is increased (see Table 1). The other structure was not affected by low concentrations of SDS. The content of secondary structures is diminished at the higher concentration of SDS (9 mM) and the amount of other structure is increased that may accompany with unfolding state for apo hTF.

Now the tertiary structures of apo hTF upon interaction with SDS at low concentration (0.5 mM) will be considered by DSC technique to get more information on domain analysis. Fig. 2 shows thermal profile of apo hTF in the absence (a) and presence of 0.5 mM concentration of SDS (b). Each curve shows a similar pattern with two apparent thermal transitions. The left and the right apparent transitions are belonging to C and N domains in DSC profile, respectively [31]. The thermal profile (b) shows the destabilisation for apo hTF in the presence of 0.5 mM SDS, because of reducing melting points (T_m's) about 5 °C for each domain (C and N) that is also accompanying with decrement of asymmetry position of C and N transitions.

Table 1
The percentage of secondary structures of apo hTF in the absence and the presence of SDS

[SDS], mM	α-Helix	β-Sheet	Other structure
0.0	32.6	28.3	39.1
0.5	28.5	36.4	39.1
1.5	18.3	42.7	39
9.0	10	9	81

Fig. 3 shows the deconvoluted C_p excess ($\langle C_p \rangle$) of apo hTF in the presence of SDS. The figure shows apo hTF in the presence of SDS (0.5 mM) having four subpeaks (like apo hTF in the absence of SDS [42]) that is, two subpeaks for C domain and other two subpeaks for N domain. The area under $\langle C_p \rangle$ and the top of the curve of thermal unfolding indicating the enthalpy of unfolding (ΔH_u) and melting point (T_m) of protein or domains, respectively. The amount of ΔH_u for all subpeaks is generally diminished during the presence of SDS especially for N domain (see Table 2). Therefore, these results show the higher effect of SDS

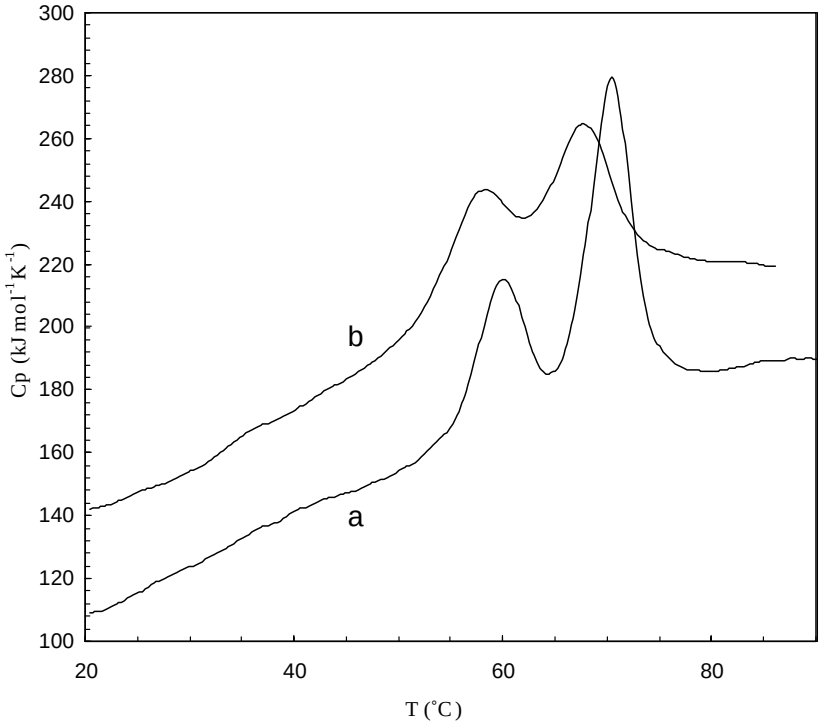

Fig. 2. DSC profiles of apo hTF in the (a) absence of SDS and (b) presence of 0.5 mM concentration of SDS.

on N domain (subpeak IV, see Fig. 3) relative to C domain of apo hTF. The results show in the presence of SDS subpeaks I, III (belonging to C and N domains, respectively) and subpeaks II, IV (belonging to C and N domains, respectively) are energetically more near similar, whereas the cited subpeaks are not identical in the absence of SDS (see Table 2).

Table 2
Enthalpy and T_m for the subpeaks of apo hTF in the absence and the presence of SDS

[SDS], mM	Domains	Subpeak[a]	ΔH (kJ mol^{-1})	T_m (°C)
0.0	C	I	262.6 ± 3.8	54
	C	II	552.6 ± 7.2	60
	N	III	363.7 ± 4.7	66
	N	IV	714.8 ± 9.3	70
0.5	C	I	328.3 ± 3.6	52
	C	II	471.0 ± 5.2	58
	N	III	323.3 ± 3.6	65
	N	IV	448.7 ± 4.9	68

[a] See Fig. 3.

For better resolution between C and N domains among interaction with SDS, the average α-helix propensity ($\langle H_D \rangle$) for C and N domains was calculated. The calculated results are shown in Table 3. The amount of $\langle H_D \rangle$ for N domain is higher than C domain that is equal to 0.6249 and 0.5771, respectively. This finding is consisted with literature [43]. The average hydrophobicity ($\langle H_\phi \rangle$) for N and C domains were also calculated by using Kyte and Doolitle scale [37]. The values of $\langle H_\phi \rangle$ for N and C domains are equal to −0.3378 and −0.4831, respectively.

Table 3
Calculated amounts of hydrophobicity, average hydrophobicity and helix propensity for N and C domains of apo hTF

Parameter	N domain	C domain
Number of residues	336	343
Hydrophobicity	−113.5	−165.7
Average hydrophobicity ($\langle H_\phi \rangle$)	−0.3378	−0.4831
Average helix propensity ($\langle H_D \rangle$)	0.6289	0.5771

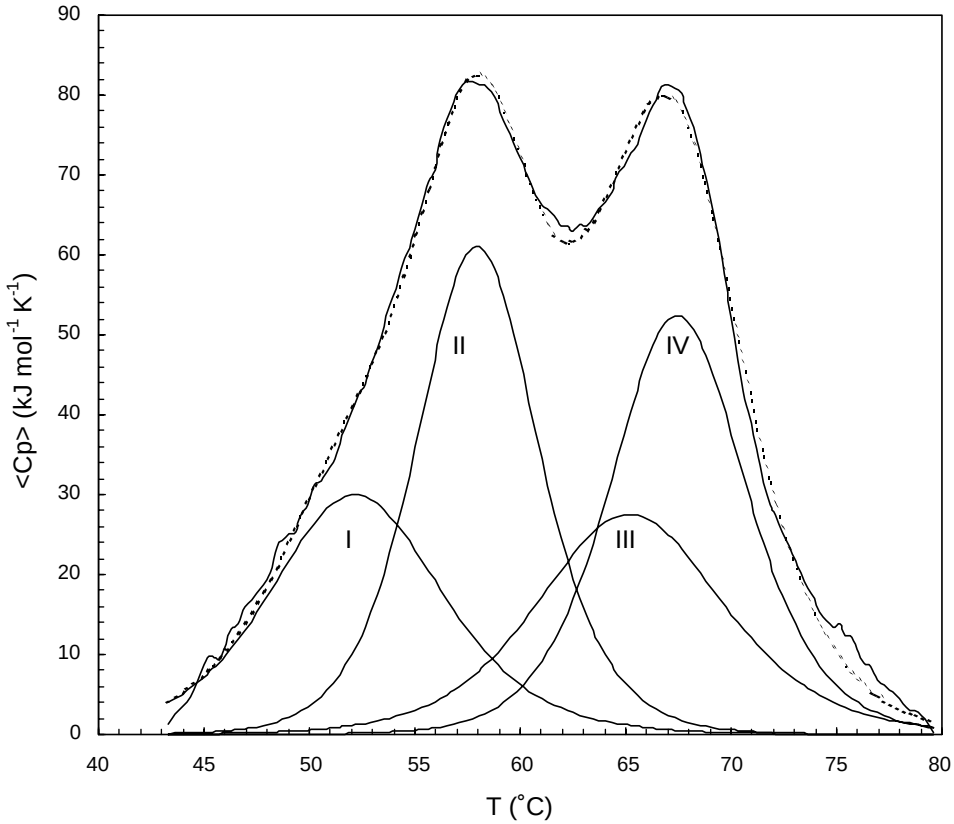

Fig. 3. Deconvoluted excess molar heat capacity of apo hTF in the presence of 0.5 mM concentration of SDS. Subpeaks of I, II and III, IV are belonging to C and N domains, respectively, (—) experimental curve and (- - -) calculated curve.

The corresponding amounts for hydrophobicity are also equal to −113.5 and −165.7, respectively. The extent of hydrophobicity is corresponded to less negative amount. Therefore, higher hydrophobicity of N domain relative to C domain indicates the higher stability for N transition than C form that is consistent with DSC data (see Fig. 2).

The results show more hydrophobicity, α-helix content, stability and hidden nonpolar group (because of ΔH_u for N domain is higher than C domain) for N domain relative to C domain. The interaction of SDS on apo hTF is predominating for N domain relative to C domain. The reduction of thermal profile area for C and N transitions and also the baseline shift in the presence of SDS (Fig. 2 profile b) relative to the absence of SDS (profile a), show that SDS was induce the more accessibility of hydrophobic residues into water that is similar to other proteins [44]. SDS interacts with protein in two steps, electrostatic and hydrophobic interactions; so first, the electrostatic interactions and then hydrophobic contribution were occurred [3]. Here, 0.5 mM concentration of SDS is chosen because the concentration of SDS be lower than the $[SDS]_{1/2}$ ($[SDS]_{1/2}$ is the concentration of SDS that is required for unfolding of the 50% of the protein sample) (data not shown). The interaction of protein with SDS at low concentrations especially below $[SDS]_{1/2}$ is in the range of electrostatic contribution [3]. Therefore, interaction of SDS with the lobes of apo hTF in the range of 0.5 mM is predominantly electrostatic interaction between negative charge of surfactant with positive charge of any domains (N, C). The results show higher affinity of N domain upon interaction with SDS, on the other hand, our calculation shows N domain

having more α-helix content (see Table 3) and that is consisted with literature [43]. The crystallographic data for apo hTF have also shown that each domain consists of a mixed β-sheet overlaid with α-helices. This folding pattern of transferrins is particularly important since the N termini of many α-helices are directed towards the central cleft of binding site and the partial positive charges they carry help to attract anions into binding cleft [32]. Then SDS as an anionic surfactant at low concentrations through electrostatic portion is interacted with apo hTF and attracted by N domain predominantly relative to C domain. This interaction leads to more diversion between α-helix and β-sheet regions due to conversion of α-helix to β-sheet. Inhibition of positive charge on the surface of apo hTF induced the new conformational structure including two more similar domains than native protein.

4. Conclusion

SDS acts as a suitable probe upon interaction with apo hTF for resolution between N and C domains. Here, SDS at low concentrations mostly electrostatically interacted with apo hTF and induces more discrepancy between α-helix and β-sheet regions. SDS having higher affinity of interaction with N domain relative to C domain, because of higher content of α-helix and partial positive charges on the surface area of N domain. The results show the energetic domains of apo hTF be degenerate due to the electrostatic interaction between SDS and apo hTF. Therefore, it can be concluded that electrostatic contribution in apo hTF induced the discrepancy between the heat content of two domains (C, N). The calculated content of hydrophobicity indicated that because of higher content of hydrophobicity, N domain has more stability than C domain. It is important to note that the higher thermal stability of N domain is remaining in the presence of low concentration of SDS due to not main effect on hydrophobic part.

Acknowledgements

The financial support from Research Council of the University of Tehran is gratefully acknowledged.

References

[1] M.N. Jones, P. Manley, J. Chem. Soc., Faraday Trans. 1 75 (1979) 1736.
[2] E. Tipping, M.N. Jones, H.A. Skinner, J. Chem. Soc., Faraday Trans. 1 70 (1974) 1276.
[3] K. Nazari, A.A. Saboury, A.A. Moosavi-Movahedi, Thermochim. Acta 272 (1997) 131.
[4] A.K. Bordbar, A.A. Moosavi-Movahedi, Bull. Chem. Soc. Jpn. 69 (1996) 2231.
[5] A.A. Saboury, A.K. Bordbar, A.A. Moosavi-Movahedi, J. Chem. Thermodyn. 25 (1996) 1077.
[6] A.K. Bordbar, A.A. Saboury, M.R. Housaindokht, A.A. Moosavi-Movahedi, J. Colloid Interf. Sci. 192 (1997) 415.
[7] A.A. Saboury, A.K. Bordbar, A.A. Moosavi-Movahedi, Bull. Chem. Soc. Jpn. 69 (1996) 2731.
[8] J.A. Reynolds, C. Tanford, J. Biol. Chem. 285 (1970) 5161.
[9] M. Levitt, Biochemistry 17 (1997) 4247.
[10] A.A. Moosavi-Movahedi, M.N. Jones, G. Pilcher, Int. J. Biol. Macromol. 10 (1988) 75.
[11] A.A. Moosavi-Movahedi, M.N. Jones, G. Pilcher, Int. J. Biol. Macromol. 11 (1989) 30.
[12] M.N. Jones, A. Finn, A.A. Moosavi-Movahedi, B. Waller, Biochim. Biophys. Acta 913 (1985) 395.
[13] M.N. Jones, Biochim. Biophys. Acta 491 (1977) 121.
[14] Y. Nǫzaki, J.A. Reynolds, C. Tanford, J. Biol. Chem. 289 (1974) 4452.
[15] M. Yamasaki, H. Yano, K. Aoki, Int. J. Biol. Macromol. 14 (1992) 275.
[16] P. Aisen, I. Listowsky, Annu. Rev. Biochem. 49 (1980) 357.
[17] N.D. Chasteen, R.C. Woodworth, Iron Transport and Storage, CRC Press, Boca Raton, FL, 1990, p. 68.
[18] R.R. Crichton, Adv. Protein Chem. 40 (1990) 281.
[19] D.C. Harris, P. Aisen, Iron Carriers and Iron Proteins, VCH, New York, 1989, p. 239.
[20] R.T.A. MacGillivray, E. Mendez, S.K. Sinha, M.R. Sutton, J. Lineback-Zins, K. Brew, Proc. Natl. Acad. Sci. USA 79 (1982) 2904.
[21] S.A. Moore, B.F. Anderson, C.R. Groom, M. Haridas, E.N. Baker, J. Mol. Biol. 274 (1997) 222.
[22] A. Rawas, H. Muirhead, J. Williams, Acta Crystallogr. D 52 (1996) 631.
[23] R.T.A. MacGillivray, S.A. Moore, J. Chen, B.F. Anderson, H. Baker, Y. Luo, M. Beweley, C.A. Smith, M.E.P. Murphy, Y. Wang, A.B. Mason, R.C. Woodworth, G.D. Brayer, E.N. Baker, Biochemistry 37 (1998) 7919.
[24] J.G. Grossmann, J.B. Crawley, R.W. Strange, K.J. Patel, L.M. Murphy, M. Neu, R.W. Evans, S.S. Hasnain, J. Mol. Biol. 279 (1998) 461.
[25] S.L. Mocklonburge, R.J. Donohoe, G.A. Olah, J. Mol. Biol. 270 (1997) 739.
[26] E.N. Baker, P.F. Lindley, J. Inorg. Biochem. 47 (1992) 147.
[27] K. Mizutani, H. Yamashita, H. Kurokawa, B. Mikami, M. Hirose, J. Biol. Chem. 274 (1999) 10190.
[28] L.N. Lin, A.B. Mason, R.C. Woodworth, J.F. Brandts, Biochemistry 30 (1991) 11660.
[29] A. Brown-Mason, S.A. Brown, N.D. Butcher, R.C. Woodworth, Biochem. J. 245 (1987) 103.

[30] A. Brown-Mason, R.C. Woodworth, J. Biol. Chem. 259 (1984) 1866.
[31] L.N. Lin, A.B. Mason, R.C. Woodworth, J.F. Brandts, Biochemistry 33 (1994) 1881.
[32] H. Sun, H. Li, P. Sadler, J. Chem. Rev. 99 (1999) 2517.
[33] L.N. Lin, A.B. Mason, R.C. Woodworth, J.F. Brandts, Biochem. J. 293 (1993) 784.
[34] P.L. Privalov, S.A. Potekhin, Meth. Enzymol. 131 (1986) 4.
[35] Y.H. Chen, J.T. Yang, H.M. Martinez, Biochemistry 11 (1972) 4120.
[36] C.N. Pace, J.M. Scholts, Biophys. J. 75 (1998) 422.
[37] J. Kyte, R.F. Doolitle, J. Mol. Biol. 157 (1982) 105.
[38] P. Manavalan, W.C. Johnson Jr., Nature 275 (1983) 831.
[39] M. Levitt, C. Chothia, Nature 301 (1976) 552.
[40] N.J. Greenfield, Anal. Biochem. 235 (1996) 1.
[41] B.V. Haeringen, F.D. Lange, I.H.M. Van Stokkum, S.K.S. Srai, R.W. Evans, R.V. Grondelle, M. Bloemendal, Proteins: Struct. Funct. Genet. 23 (1995) 233.
[42] M. Rezaei-Tavirani, A.A. Moosavi-Movahedi, A.A. Saboury, G.H. Hakimelahi, B. Ranjbar, M.R. Housaindokht, Thermochim. Acta 383 (2002) 108.
[43] H. Kurokawa, B. Mikami, M. Hirose, J. Mol. Biol. 294 (1995) 196.
[44] V.V. Loladze, D.N. Ermolenko, G.I. Makhatadze, Protein Sci. 10 (2001) 1343.